Polymer Chemistry

Accepted Manuscript

ROYAL SOCIETY OF CHEMISTRY

www.rsc.org/polymers

Polymer Chemistry

ARTICLE

Preparation of core-shell particles by surface-initiated cycloketyl radical mediated living polymerization

Received 00th January 20xx,
Accepted 00th January 20xx

DOI: 10.1039/x0xx00000x

www.rsc.org/

Xianguang Huang,[ab] Li Wang*[ab] and Wantai Yang*[ab]

A simple and novel synthetic route toward core-shell polymeric particles *via* surface-initiated cycloketyl radical mediated living polymerization (CMP) is presented. Cross-linked polymaleic anhydride/isoprene particles (CPMIP) prepared by self-stable precipitation polymerization were reacted with 9,9′-bixanthydrol (BIXANDL), which endowed them with potential initiating sites for subsequent CMP of styrene, methyl methacrylate and n-butyl acrylate. Uniform core-shell particles were successfully obtained in all cases and their sizes increased with continuous monomer conversion, demonstrating the versatility and living feature of surface-initiated CMP.

Introduction

Polymeric particles, owing to their small size, large specific surface area, high diffusivity and mobility, have gained a vast range of applications in the property optimization of polymeric materials, micro reactor, catalytic agents, chromatographic packing, microelectronics, biomedicine and biotechnology, etc.[1-5] The growing range and specificity of applications are connected to successes in preparing polymeric particles with diverse chemical compositions, morphologies and functions. Regarding morphology manipulation of polymeric particles, the production of core-shell particles has become a hot topic because they enable the combination of superior properties not possible from one single component in a simple and fine structural pattern.[4-8]

Among the diversified techniques for preparing core-shell polymeric particles,[9-45] a most common and versatile route is to graft polymer brushes by surface-initiated radical polymerization from pre-synthesized particles that bear initiator sites. This method suffers from ununiform grafted chain lengths and the inevitable formation of free ungrafted chains when conventional radical polymerization is utilized.[19,24,25] Fortunately, these drawbacks can be overcome by the introduction of the burgeoning controlled/living radical polymerization (CLRP) methods, such as nitroxide-mediated polymerization(NMP),[15-18] atom transfer radical polymerization (ATRP)[19-34] and reversible addition-fragmentation chain transfer polymerization (RAFT).[35-44] Surface-initiated CLRP makes it possible to achieve deliberate control over grafted chain length, shell thickness and structrual uniformity as well as the elimination of free homopolymer formation in the synthesis of core-shell particles. For instance, Chevignyet al.[15] obtained well-defined core-shell SiO_2/PS particles by binding alkoxyamine to the surfaces of SiO_2 particles followed by conducting NMP of styrene. Jhaveri et al.[26] demonstrated the versatility of surface-initiated ATRP by generating a number of different polymeric shell/ poly(methyl methacrylate) core particles and judging from scanning electron microscope observations, they thought that there was no free polymer grown in solution. You et al.[36] prepared dendritic core/temperature-sensitive shell (poly(N-isopropylacrylamide)) particles through a three-step route *via* RAFT. The molecular weight of the core-shell particles increased almost linearly with increasing conversion of N-isopropylacrylamide, and a narrow polydispersity index of about 1.2 was achieved. Another benefit of surface-initiated CLRP is that it endows core-shell particles with a wide variety of opportunities for subsequent chain-end functionalization or block-copolymerization due to the preservation of high chain-end functionality.[28] Zheng et al.[21] synthesized core-shell poly(divinylbenzene)/polystyrene and poly(divinylbenzene) /poly(styrene-b-4-methyl-styrene) particles by the hydrochlorination of the surface vinyl groups of poly(divinylbenzene) particles and subsequent ATRP using CuBr/2bipy catalyst system. The success in grafting a block copolymer demonstrated the living nature of surface-initiated ATRP.

Despite the successes in preparing core-shell particles with living radical polymerization methods, we have to face the inherent drawbacks and limitations of each method. NMP system suffers from its high cost of reagents and requirement for relatively high reaction temperature. ATRP system contains toxic transition metal salts that are difficult to remove. RAFT system induces increased toxicity, unpleasant odor and color of products due to the use of thiocarbonylthio compounds.

[a] TheState Key Laboratory of Chemical Resource Engineering, Beijing,100029, China.
[b] Collegeof Materials Science and Engineering, Beijing University ofChemical Technology, Beijing, 100029, China. Email: lwang@mail.buct.edu.cn; yangwt@mail.buct.edu.cn. Fax:+86-010-64416338

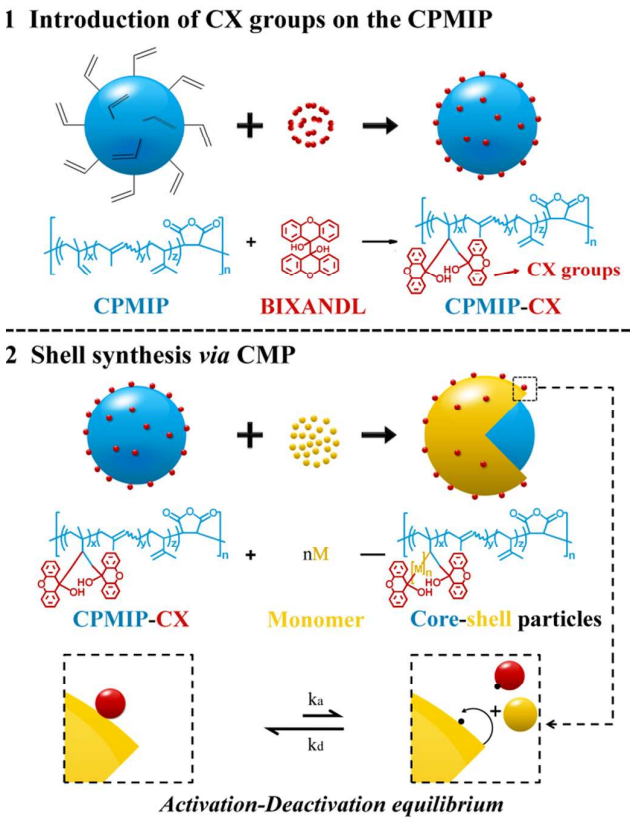

Scheme 1 Schematic illustration of the synthesis of core-shell particles by surface-initiated cycloketyl radical mediated living polymerization.

Thus, further improvements in the synthetic techniques for core-shell particles rely greatly on advances in CLRP methods.

In our previous work, we have developed a novel CLRP method called cycloketyl radical mediated living polymerization (CMP).[46] It is based on the use of 9,9'-bixanthene-9,9'-diol (BIXANDL), which produces cycloketyl xanthone (CX) radicals readily after homolytic cleavage under thermal or photo stimuli. The CX radicals can initiate and control the radical polymerization of common monomers, manifesting good controlled/living features. The greatest merit of CMP is that it is a simple mono-component and metal/odor/color free method. This endues CMP with inherent advantage for large-scale industrial production.

The present work applies CMP to the preparation of core-shell particles. The synthetic strategy is illustrated in Scheme 1. First, cross-linked polymaleic anhydride/isoprene particles (CPMIP) were prepared by a self-stable precipitation polymerization process developed in our lab.[47-49] Then, by heating the CPMIP and BIXANDL together, the addition reaction of CX radicals to the vinyl groups on the surfaces of the CPMIP took place, yielding the CPMIP bearing surface CX dormant groups (CPMIP-CX). Finally, the graft polymerization of three typical monomers (styrene, methyl methacrylate and n-butyl acrylate) from the CPMIP was conducted in tetrahydrofuran (THF) or isopentyl acetate (IPA) which were good solvents of the polymers. Uniform core-shell particles were successfully obtained in all cases. Therefore, our research provides a simple and environment-friendly method with application prospect in preparing core-shell particles. Meanwhile, the livingness of CMP was proven.

Experimental

Mateirals

Methyl methacrylate (MMA, 98%), styrene (St, 98%) and n-butyl acrylate (BA, 98%) were purchased from Beijing Yili Fine Chemical Co., Ltd. and distilled under reduced pressure to remove the inhibitor prior to use. Maleic anhydride (MAH, AR), 2, 2'-azobisisobutyronitrile (AIBN, AR), isopentyl acetate (AR) and tetrahydrofuran (THF, AR) were supplied by Beijing Sinopharm Reagent Co., Ltd. and used as received. Isoprene (IP, 98%) was provided by Alfa Aesar Chemical Co., Ltd. and used as received. 9,9'-bixanthydrol (BIXANDL) was prepared in our lab according to the literature method[46] and purified before use.

Synthesis of the CPMIP

The CPMIP were prepared by the self-stable precipitation polymerization. Thus, 0.1 mol of MAH was dissolved in 75 mL of IPA and 25 mL of n-hexane in a three-necked flask (500 mL), followed by the addition of 0.1 mol of IP and 0.33 g of AIBN. Then the flask was purged with nitrogen. Subsequently, the solution was stirred at 70 °C for 6 h. The resulting mixture was centrifugated and washed with ethanol repeatedly. The product was dried at 50 °C in a vacuum oven and the yield was approximately 70%.

Introduction of CX groups on the CPMIP

In a dried flask, 5 g of the CPMIP was dispersed homogeneously in 50 g of THF assisted by sonication, followed by the addition of 1 g of BIXANDL. Then the flask was degassed and backfilled with nitrogen by three freeze-pump-thaw cycles. The reaction proceeded at 60 °C in a water bath for 6 h. The resulting mixture was centrifugated and washed with THF repeatedly. The product CPMIP-CX was dried at room temperature in a vacuum oven.

Shell synthesis via CMP

In a dried flask, desired amount of the CPMIP-CX was dispersed homogeneously in solvent, followed by the addition of monomer. Then the flask was degassed and backfilled with nitrogen by three freeze-pump-thaw cycles. The formulations and polymerization conditions are listed in Table 1. During the polymerization, samples (m_1) were taken out from the flask periodically. After the addition of trace amounts of inhibitor to stop the polymerization, the samples were dried until a constant weight (m_2) was reached. The conversion of monomer was determined by gravity using the following equation:

$$C = \frac{m_2 - m_1 \times A}{m_1 \times B}$$

where A is the weight fraction of the CPMIP-CX and B is the weight fraction of monomer.

Characterization

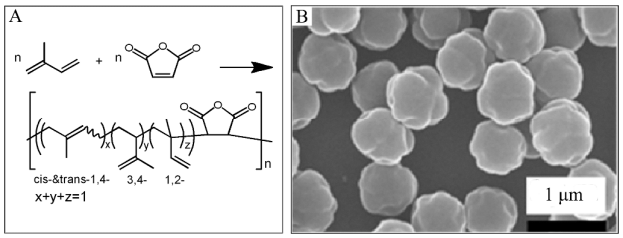

Fig.1 Synthesis (A) and FESEM micrographs (B) of the CPMIP

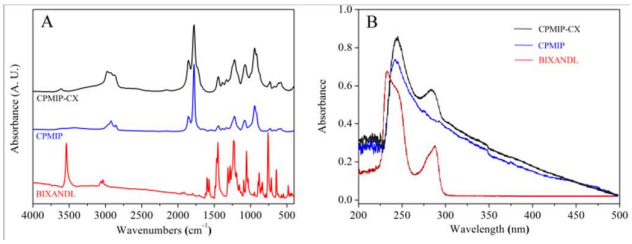

Fig.2 FTIR (A) and UV-vis (B) spectra of the CPMIP-CX. Spectra for relevant CPMIP and BIXANDL are shown for comparison.

The molecular structure of the particles was characterized using a Nicolet Nexus670 fourier transform infrared spectroscope (FTIR, USA) and a GBC Cintra 20 ultraviolet-visible spectrophotometer (Australia). The morphology of the particles was observed using a Hitachi-S4700 field emission scanning electron microscope (FESEM, Japan) and a Hitachi-800-1 transmission electron microscope (TEM, Japan). Particle size analysis was carried out on the FESEM micrographs using an image processing software. Generally, the diameters of 100 particles were measured and substituted into the following equations to calculate the average diameter (Dn), coefficient of variation (CV), average volume (Vn) and grafting efficiency (GE):

$$Dn = \frac{\sum_{i=1}^{n} d_i}{n} \quad CV = \sqrt{\frac{\sum_{i=1}^{n}(d_i - Dn)^2}{n-1}} \Big/ Dn$$

$$Vn = 4\pi(Dn/2)^3/3$$

$$GE = \frac{m_{shell}}{m_{core}}\frac{m_{core}}{m_{all}} = \frac{\rho_2 4\pi[(Dn/2)^3 - (D0/2)^3]/3}{\rho_1 4\pi(D0/2)^3/3}\frac{1}{fC}$$

where n is the number of the particles, d_i is the diameter of the i^{th} particle, D0 and $\rho_1$are the initial diameter and density of the CPMIP-CX, ρ_2 is the density of the grafted polymer, f is the weight ratio of monomer to the CPMIP-CX and m_{all} is the weight of all polymerized monomer.

Results and discussion

Introduction of CX groups on the CPMIP

Monodispersed CPMIP were used as seed particles for surface-initiated CMP. They were prepared by the self-stable precipitation polymerization developed in our lab.[48-50] This method requires no addition of any stabilizer and produces well-defined particles with their sizes being readily controllable by varying polymerization time and formulations. Fig.1B shows the FESEM micrographs of the CPMIP. These particles were pumpkin-like and quite uniform in size with a Dn of 820 nm and a CV of 6.8%. According to the literature,[50] MAH and IP have a strong tendency to copolymerize in an alternate fashion due to the donor-acceptor characteristic of them. In the present work, the alternating copolymerization and precipitation of the yielded copolymer from solvent led to the formation of the CPMIP. It should be noted that the consumption of all double bonds of IP was impossible during the copolymerization. Plenty of double bonds with various configurations[13,50] (cis-1,4-, trans-1,4-, 1,2- and 3,4-, shown in Fig. 1A) must be left in the CPMIP, which enabled the subsequent introduction of CX groups.

CX groups were introduced by heating the CPMIP in THF with BIXANDL. During this reaction, the CX radicals produced after the decomposition of BIXANDL added to the double bonds of the CPMIP, thus forming the CPMIP-CX. Fig. 2 shows the FTIR and UV-vis spectra of BIXANDL, CPMIP and CPMIP-CX. In the FTIR spectrum of BIXANDL, the sharp and strong peak at 3537 cm^{-1} was assigned to the stretching vibration of the hydroxyl groups; the peaks at 3060, 1450 & 760 cm^{-1} corresponded to the absorption of benzene rings and the peaks at 1234 & 1057 cm^{-1} were assigned to the stretching vibration of C-O-C & C-OH bonds. For the CPMIP, the characteristic absorptions of CH_2 and anhydride groups showed up at 2930 and 1778 cm^{-1}, respectively. In the FTIR spectrum of the CPMIP-CX, both the characteristic peaks of the CPMIP-CX and a weak peak assigned to the stretching vibration of hydroxyl groups could be discerned, indicating that the CPMIP-CX contained the CMP initiator fragments. The CPMIP and CPMIP-CX (dispersed in THF) were subjected to UV-Vis spectroscopy and the results are given in Fig. 2B. BIXANDL showed two absorption peaks at 288 (B band) and 243 nm (E_2 band), while the CPMIP had a broad absorption band at around 230-350 nm. The UV spectrum of the CPMIP-CX exhibited a slight blue shift of the characteristic absorption of BIXANDL (288 nm) to 284 nm. This confirms that the CX groups were successfully introduced on the CPMIP.

One important question about the CX groups is their exact location in the CPMIP-CX. From a kinetic view, BIXANDL should preferentially react with the surface double bonds of the CPMIP because of their cross-linked nature. Thus, most of the CX groups should be located in the outer layer of the particles. Zheng et al.[21] carried out hydrochlorination of the pendant vinyl groups of PDVB particles to introduce ATRP initiator sites. They believed that the hydrochlorinated layer showed its own gradient due to the cross-linking gradient of PDVB particles and the penetration of hydrogen chloride into the particles. Ultimately, they reached a conclusion that the ATRP initiator sites could be found at least 100 nm from the surface. Our case was similar to that of Zheng et al. Thus, we tend to believe that at least a thin outer layer of the CPMIP-CX contained the CMP initiator sites. The inner cores of the CPMIP-CX might be free of the CX groups because the cross-linked structure hindered the diffusion and reaction of BIXANDL. Another question worth addressing is the selectivity of the reaction between BIXANDL and the remaining double

bonds with various configurations. It is difficult to identify the configurations of the double bonds and their changes after the reaction from FTIR results. This is because a strong and broad band (850-1020 cm^{-1}) assigned to anhydride groups overlapped with the characteristic bands of the double bonds with 1,2- and 3,4- configurations.NMR analysis also failed due to the cross-linked nature of the CPMIP. The work of Shao et al.[51] can be taken as a reference. They carried out the thiol-ene 'click' reaction of mercaptoethanol with the double bonds of polyisoprene through a radical mechanism. They found that the reaction occurred only on the double bonds with 1,2-configuration. This might be due to the fact that the other configurations had greater steric hindrance for the reaction to occur. Therefore, it can be inferred that BIXANDL had a higher possibility to add to the pendant vinyl groups (1,2-configuration). In summary, subsequent shell growth was initiated most probably from the CX groups anchored to the pendant vinyl groups (1, 2- configuration) in the outer layer of the CPMIP.

PS shell growth via CMP

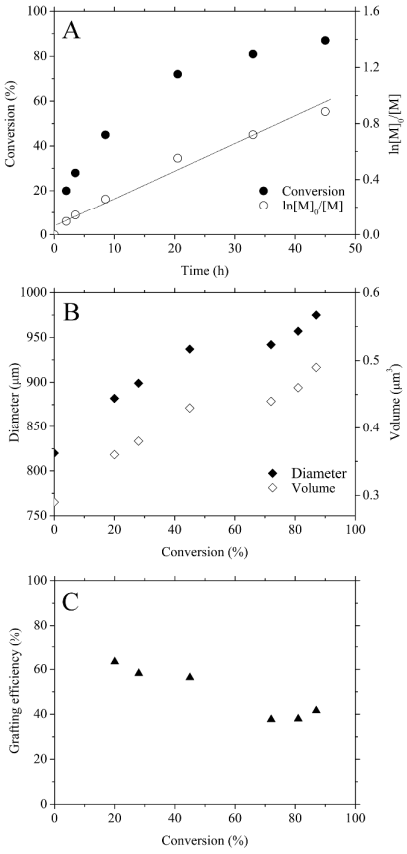

Fig.3 Plots of the conversion of St and $ln[M]_0/[M]$ *vs.* polymerization time (A), plots of average particle diameter (Dn) and volume (Vn) *vs.* the conversion of St (B) and plot of grafting efficiency *vs.* the conversion of St (C)

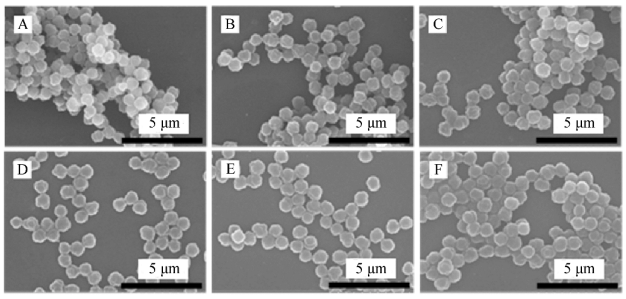

Fig.4 FESEM micrographs of the core-shell CPMIP-CX/PS particles at increasing conversion of St: (A)20%; (B) 28%; (C) 45%; (D) 72%; (E) 81% and (F)87%

The graft polymerization of St from the CPMIP-CX was carried out in THF at 70 ^{o}C for 45 h. The weight ratio of CPMIP-CX/St/THF was 1:2:10. Small amounts of samples were taken out from the polymerization system periodically to gain a clear insight into the growing process of the core-shell particles. Fig. 3A gives the plots of the conversion of St and $ln[M]_0/[M]$ *vs.* polymerization time. The conversion of St increased at a slower rate in comparison with conventional radical polymerization, reaching 45% in 8.5 h. As time went on, the polymerization slowed down gradually and a conversion of 87% was attained in 45 h. The plot of $ln[M]_0/[M]$ *vs.* time exhibited almost linear relationship with a correlation factor of 0.975. This typical first order kinetics concerning the monomer concentration points to constant radical concentration during the polymerization, which implies that the grafted PS chains probably grew in a controlled fashion. Such behavior was also reported by many researchers in conducting surface-initiated CLRP.[19,20,24,28] Unfortunately, it was impossible to measure the evolution of the Mn and PDI of the grafted PS chains directly because of their covalent linkages to the CPMIP-CX cores.

Fig. 4 shows the FESEM micrographs of the particles at different conversion of St. It can be seen that the particles increased in size gradually and remained uniform in shape with increasing conversion of St. The FESEM micrographs were analyzed using an image processing software to estimate Dn, CV & Vn and the results are plotted in Fig. 3B. Dn increased with increasing conversion of St, for example, from 820 to 937 nm at a conversion of 45%, then reached 975 nm at a conversion of 87%. This corresponds to an almost linear growth of Vn with increasing conversion of St. The Vn values at 0, 45 and 87% conversion of St were 0.29, 0.43 and 0.49 μm^3, respectively. It should be noted that THF is a good solvent of PS, thus the precipitation of PS onto particle surface can be excluded and the volume increase can merely be attributed to surface graft polymerization. Assuming the selective conversion of St into surface-grafted PS chains, the linear growth of Vn with the conversion of St is rational. In the literature on surface-initiated CLRP, particle diameter and volume were often plotted against polymerization time and different increasing trends were reported. Holzinger et al.[19,20] synthesized metal-oxide-core polymer-shell nanoparticles by surface-initiated ATRP and observed a linear growth of particle diameter. By contrast, Zheng et al.[22] and Barner et al.[37]

observed a size jump at the initial stage, followed by a slower and linear growth with polymerization time. They believed that the rapid size increase at early stages might be due to quick polymerization of monomer within the outer layer of swollen lightly cross-linked core particles, followed by quick solvent swelling. As time went on, the growth in particle size was hampered by the diffusion of monomer into the network structure of the core particles. We believe that the apparent linear growth of particle diameter with time in the former report was because the conversion of monomer was quite low. The increase of Vn with polymerization time (not shown) in our case assembled the latter report. Therefore, the size of the core-shell particles can be readily controlled by simply adjusting polymerization time.

It is surprising that the statistical CV (not shown) of the core-shell particles was maintained at around only 6% during the polymerization, indicating fairly good monodispersibility. This circumstantial evidence supports the controlled/living features of surface-initiated CMP. Jhaveriet al.[26] successfully carried out surface-initiated ATRP from corss-linked PMMA cores and obtained core-shell particles with a narrow distribution. They believed that the narrow distribution of particle sizes may be attributed to the living feature of brush growth via ATRP. In other words, ATRP can produce grafted chains with uniform lengths, which may guarantee the uniformity of the shell thickness. According to our previous work,[35] the CX radicals have high deactivation reactivity with chain radicals, endowing CMP with good controlled/living features in solution polymerization. This may played a great role in obtaining the core-shell CPMIP-CX/PS particles with a narrow distribution.

The internal structure of the core-shell particles was directly observed by TEM. A representative micrograph is given in Fig. 5, and white dashed lines were drawn to separate the particles from background. The particle size in the TEM micrograph confirmed the FESEM observations and a core-shell architecture can be clearly distinguished. The dark phase was assigned to the CPMIP-CX cores, while the light circular phase corresponded to the grafted PS shells. It should be noted that the transition from core to shell was not sharp (ambiguous interface), but in a gradual manner. This indicates the initiation of St from within the outer layer of the CPMIP-CX and partial mixing of PS with the network structure of the core particles.

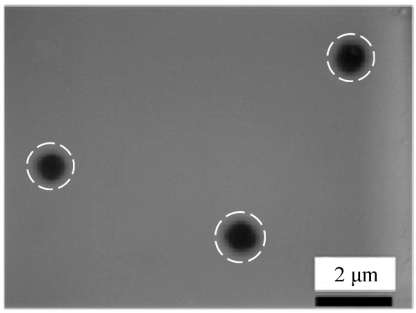

Fig.5 TEM micrograph of the core-shell CPMIP-CX/PS particles

The clear core-shell structure and the linearly growth of particle volume during a long polymerization time definitely show the controlled/living feature of the system. The mechanism of the surface-initiated CMP from the CPMIP-CX is illustrated in Scheme 1. Under thermal stimuli, the CX groups disassociated from the CPMIP-CX, producing CPMIP surface radicals and CX radicals which stayed in solution. The addition of St in solution to the former radicals led to the formation of the surface-grafted PS chain radicals. Then, after a persistent radical effect, an activation-deactivation equilibrium between the surface-grafted PS chain radicals and the CX radicals was established and maintained, which made the particles grow in a controlled/living mode.

Because the CX radicals in solution also had initiation reactivity, though small, it could initiate the polymerization of St in solution. Similarly, an activation-deactivation equilibrium between the homopolystyrene chain radicals and the CX radicals in solution was built. Obviously, from a kinetic view, the propagation rate of the chain radicals in solution would be larger than that of the surface-grafted chain radicals. Therefore, the homopolymerization would take up a higher and higher proportion. Figure 3C shows the grafting efficiency (GE) defined as the percentage of grafted polymer in all polymerized monomer. It can be observed that GE was over 60% at the early stage of graft polymerization and then decreased to below 40% gradually with increasing conversion of St.

Synthesis of different polymeric shells

Two other typical monomers (MMA and BA) were also used to prepare core-shell particles with THF and IPA as polymerization medium (good solvent), aiming to evaluate the versatility of this method. The formulations, polymerization conditions and main results of shell synthesis using different monomers are summarized in Table 1, Fig. 6 and Fig. 7. It took 7.5 and 9.4 h for the conversion of MMA and BA to reach 84% and 82%, respectively. Therefore, the order of the polymerization rate of different monomers in surface-initiated CMP was MMA > BA > St. The linear fitting of $\ln[M]_0/[M]$ *vs.* time for MMA and BA gave correlation factors of 0.999 and 0.940. Thus, the surface-initiated CMP of MMA and BA showed typical first order kinetics concerning the monomer concentration, which was similar to the case of St.

Fig. 6 B & D show the plots of Dn and Vn *vs.* the conversion of monomer for the synthesis of PMMA and PBA shells. Under both circumstances, Dn and Vn grew with the continuous conversion of monomer. For MMA, Dn and Vn increased by 100 nm and 0.11 μm^3 at a conversion of 38%, then increased by 137 nm and 0.17 μm^3 at a conversion of 84%. Similarly, Dn and Vn raised by 103 nm and 0.12 μm^3 at 59% conversion of BA, then raised by 127 nm and 0.15 μm^3 when 82% conversion of BA was achieved. Vn increased almost linearly with monomer conversion in the case of BA, while the linear relationship was poorer for MMA. Besides, the CV of the CPMIP-CX/PMMA and CPMIP-CX/PBA particles did not exceed 7%, suggesting good monodispersibility of the core-shell

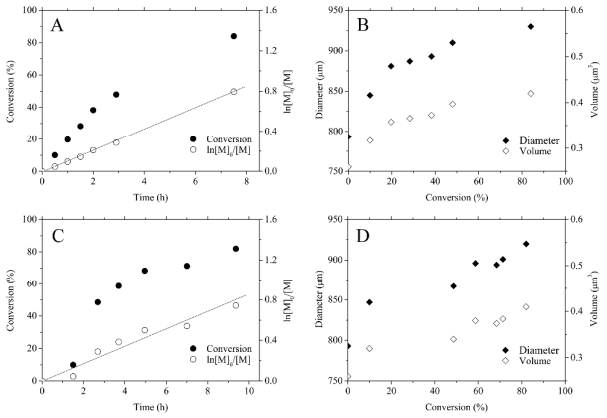

Fig.6 Synthesis of PMMA (A & B) and PBA (C & D) shells: plots of the conversion of monomer and $\ln[M]_0/[M]$*vs*. polymerization time (A& C) and plots of average particle diameter (Dn) and volume (Vn) *vs*. the conversion of monomer (B & D)

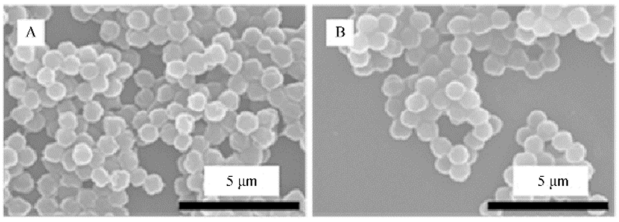

Fig.7 FESEM micrographs of the core-shell CPMIP-CX/PMMA (A) and CPMIP-CX/PBA (B) particles

particles. This is well illustrated in the FESEM micrographs of the final core-shell particles, which are shown in Fig. 7. In summary, these results confirm the versatility of surface-initiated CMP, which is an environmental-friendly method demonstrating characteristics of controlled/living radical polymerization and maintaining fairly good control over the size and uniformity of core-shell particles.

Further research will be focused on the expansion of shell materials to functional polymers, such as stimuli-sensitive polymers. Multiple surface-initiated CMP to prepare core-shell particles with multilayer architecture may also be considered.

Conclusions

We have demonstrated a simple, feasible and environmental-friendly method called surface-initiated CMP in preparing core-shell particles with uniform and controllable size. By planting CX groups on the surface of the CPMIP, we can obtain particles with initiator sites for subsequent shell synthesis via CMP. Monodispersed core-shell particles have been obtained when using St for shell synthesis, and their size can be readily controlled by simply adjusting reaction time. Excellent results have also been obtained for the synthesis of PMMA and PBA shells. Therefore, our method provides a versatile approach with application prospect in the design and production of a rich diversity of core-shell particles.

Acknowledgements

This research is financially supported by the Natural Science Foundation of China (no. 21404004) and Fundamental Research Funds for the Central Universities of China (no. ZY1409).

Notes and references

1 J. M. Asua, Polymeric dispersions. Principles and applications. Dordrecht: Kluwer, 1997.
2 P. A. Lovell and M. S. El-Aasser, Emulsion polymerization and emulsion polymers. Chichester: Wiley, 1997.
3 W. H. Zhang, Y. Huang and W. Tian, *Prog. Chem*., 2013, **25**, 1951.
4 S. S. Cao, J. R. Chen and J. Hu, *Aust. J. Chem*., 2009, **62**, 1561.
5 R. A. Ramli, W. A. Laftah and S. Hashim, *RSC Adv*., 2013, **3**, 15543.
6 T. Borase, M. Iacono, S. I. Ali, P. D. Thornton and A. Heise, *Polym. Chem*., 2012, **3**, 1267.
7 K. P. McNamee, L. M. Pitet and D. M. Knauss, *Polym. Chem*., 2013, **4**, 2546.
8 X. Z. Kong, W. Q. Jiang, X. B. Jiang and X. L. Zhu, *Polym. Chem*., 2013, **4**, 5776.
9 J. Pusch and A. M. van Herk, *Macromolecules*, 2005, **38**, 6909.
10 X. Li, J. Zuo, Y. L. Guo and X. H. Yuan, *Macromolecules*, 2004, **37**, 10042.
11 C. D. Jones and L. A. Lyon, *Macromolecules*, 2000, **33**, 8301.
12 H. Li, J. Han, A. Panioukhine and E. Kumacheva, *J. Colloid Interface Sci*., 2002, **255**, 119.
13 C. Cheng, K. Qi, D. S. Germack, E. Khoshdel and K. L. Wooley, *Adv. Mater.*, 2007, **19**, 2830.
14 J. Jang, Y. Nam and H. Yoon, Adv. Mater., 2005, **17**, 1382.
15 C. Chevigny, D. Gigmes, D. Bertin, J. Jestin and F. Boué, *Soft Matter*, 2009, **5**, 3741.
16 M. Kobayashi, R. Matsuno, H. Otsuka and A. Takahara, *Sci. Technol. Adv. Mater*., 2006, **7**, 617.
17 C. Deleuze, M. H. Delville, V. Pellerin, C. Derail and L. Billon, *Macromolecules*, 2009, **42**, 5303.

Table 1 Shell synthesis *via* CMP from the CPMIP-CX

Shell	Solvent	CPMIP-CX/ monomer/solvent weight ratio	Reaction Temperature (^oC)	Reaction Time (h)	Conversion (%)	Dn (nm)	CV (%)	Volume (μm^3)
PS	THF	1:2:10	70	45	87	975	6.0	0.49
PMMA	THF	1:2.5:10	70	7.5	84	930	5.9	0.42
PBA	IPA	0.5:2:10	70	9.2	82	920	3.7	0.41

Note: the Dn, CV and volume of the CPMIP for PS shell were 820 nm, 6.8% and 0.29 μm^3, while those for PMMA and PBA shells were 793 nm, 4.7% and 0.26 μm^3, respectively.

Polymer Chemistry

ARTICLE

18 V. Ladmiral, T. Morinaga, K. Ohno, T. Fukuda and Y.Tsujii, *Euro. Polym. J.*, 2009, **45**, 2788.
19 D. Holzinger and G. Kickelbick, *Chem. Mater*., 2003, **15**, 4944.
20 D. Holzinger and G. Kickelbick, *J. Mater. Chem*., 2004, **14**, 2017.
21 G. D. Zheng and H. D. H. Stöver, *Macromolecules*, 2002, **35**, 6828.
22 G. D. Zheng and H. D. H. Stöver, *Macromolecules*, 2002, **35**, 7612.
23 K. Min, J. H. Hu, C. C. Wang and A. Elaissari, *J.Polym. Sci.: Part A: Polym. Chem*., 2002, **40**, 892.
24 B. F. Senkal and N. Bicak, *Euro. Polym. J*., 2003, **39**, 327.
25 N. Bicak, M. Gazi, G. Galli and E. Chiellini, *J.Polym. Sci.: Part A: Polym. Chem.*, 2006, **44**, 6708.
26 S. B. Jhaveri, D. Koylu, D. Maschke and K. R. Carter, *J. Polym. Sci.: Part A: Polym. Chem*., 2007, **45**, 1575.
27 K. Ishizu, N. Kobayakawa, S. Takano, Y. Tokuno and M. Ozawa, *J. Polym. Sci.: Part A: Polym. Chem*., 2007, **45**, 1771.
28 A. Kotal, T. K. Mandal and D. R. Walt, *J. Polym. Sci.: Part A: Polym. Chem*., 2005, **43**, 3631.
29 T. Morinaga, M. Ohkura, K. Ohno, Y. Tsujii and T. Fukuda, *Macromolecules*, 2007, **40**, 1159.
30 D. H. Lee, Y. Tokuno, S. Uchida, M. Ozawa and K. Ishizu, *J. Colloid Interf. Sci.*, 2009, **340**, 27.
31 K. Ohno, T. Akashi, Y. Huang and Y. Tsujii, *Macromolecules*, 2010, **43**, 8805.
32 J. L. Liang, W. W. He, L. F. Zhang, Z. B. Zhang, J. Zhu, L. Yuan, H. Chen, Z. P. Cheng and X. L. Zhu, *Langmuir*, 2011, **27**, 12684.
33 K. Ishizu, I. Amir, N. Okamoto, S. Uchida, M. Ozawa and H. Chen, *J. Colloid Interf. Sci.*, 2011, **353**, 69.
34 K. Ohno, C. Mori, T. Akashi, S. Yoshida, Y. Tago, Y. Tsujii and Y. Tabata, *Biomacromolecules*, 2013, **14**, 3453.
35 M. J. Monteiro and J. de Barbeyrac, *Macromol. Rapid Commun*., 2002, **23**, 370.
36 Y. Z. You, C. Y. Hong, C. Y. Pan and P. H. Wang, Adv. Mater., 2004, **16**, 1953.
37 L. Barner, C. E. Li, X. J. Hao, M. H. Stenzel, C. Barner-Kowollik and T. P. Davis, *J. Polym. Sci.: Part A: Polym. Chem.*, 2004, **42**, 5067.
38 Y. K. Yang, Z. F. Yang, Q. Zhao, X. J. Cheng, S. C. Tjong, R. K. Y. Li, X. T. Wang and X. L. Xie, *J. Polym. Sci.: Part A: Polym. Chem.*, 2009, **47**, 467.
39 D. C. Wan, Q. Fu and J. L. Huang, *J. Polym. Sci.: Part A: Polym. Chem.*, 2005, **43**, 5652.
40 M. J. Monteiro and J. de Barbeyrac, *Macromolecules*, 2001, **34**, 4416.
41 W. Smulders and M. J. Monteiro, *Macromolecules*, 2004, **37**, 4474.
42 T. L. U. Nguyen, B. Farrugia, T. P. Davis, C. Barner-kowollik and M. H. Stenzel, *J. Polym. Sci.: Part A: Polym. Chem.*, 2007, **45**, 3256.
43 J. Moraes, K. Ohno, T. Maschmeyer and S. Perrier, *Chem. Commun*., 2013, **49**, 9077.
44 J. Moraes, K. Ohno, G. Gody, T. Maschmeyer and S. Perrier, *Beilstein J. Org. Chem.,* 2013, **9**, 1226.
45 A. M. Imroz Ali and A. G. Mayes, *Macromolecules*, 2010, **43**, 837.
46 X. F. Zheng, M. Yue, P. Yang, Q. Li, and W. T. Yang, *Polym. Chem*., 2012, **3**, 1982.
47 C. M. Xing and W. T. Yang, *Macromol. Rapid Commun.*, 2004, **25**, 1568.
48 C. M. Xing and W. T. Yang, *J. Polym. Sci.: Part A: Polym. Chem.*, 2005, **43**, 3760.
49 C. M. Xing and W. T. Yang, *Macromol. Chem. Phys*., 2006, **207**, 621.
50 D. Contreras-López, E. Saldívar-Guerra and G. Luna-Bárcenas, *Euro. Polym. J*., 2013, **49**, 1760.
51 F. Shao, X. F. Ni and Z. Q. Shen, *Chinese Chem. Lett*., 2012, **23**, 347.

Core-shell particles were prepared by surface-initiated cycloketyl radical mediated living polymerization, which can achieve deliberate control over particle size and uniformity. It has a significant potential for industrial application.